

Article

Reactions of Experimentally Known *Closo*-C₂B₈H₁₀ with Bases. A Computational Study

Josef Holub ¹, Jindřich Fanfrlík ², Michael L. McKee ³  and Drahomír Hnyk ^{1,*} 

¹ Institute of Inorganic Chemistry of the Czech Academy of Sciences, CZ-250 68 Husinec-Řež, Czech Republic; holub@iic.cas.cz

² Institute of Organic Chemistry and Biochemistry of the Czech Academy of Sciences, CZ-166 10 Praha 6, Czech Republic; jindrich.fanfrlik@marge.uochb.cas.cz

³ Department of Chemistry and Biochemistry, Auburn University, Auburn, AL 36849, USA; mckeeml@auburn.edu

* Correspondence: hnyk@iic.cas.cz

Received: 19 August 2020; Accepted: 29 September 2020; Published: 3 October 2020

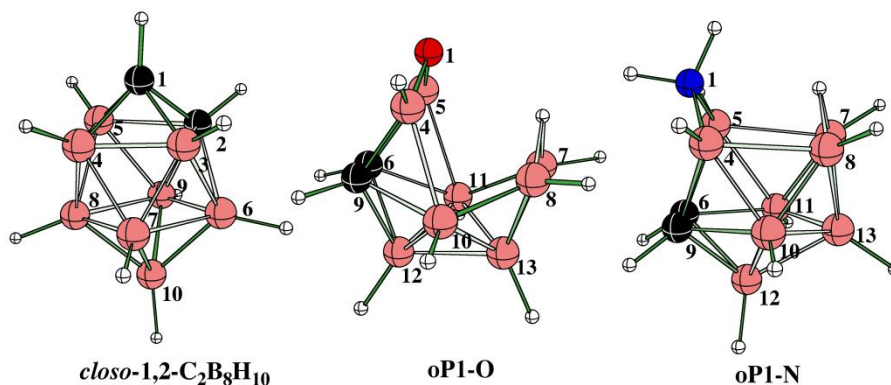


Abstract: On the basis of the direct transformations of *closo*-1,2-C₂B₈H₁₀ with OH⁽⁻⁾ and NH₃ to *arachno*-1,6,9-OC₂B₈H₁₃⁽⁻⁾ and *arachno*-1,6,9-NC₂B₈H₁₃, respectively, which were experimentally observed, the DFT computational protocol was used to examine the corresponding reaction pathways. This work is thus a computational attempt to describe the formations of 11-vertex *arachno* clusters that are formally derived from the hypothetical *closo*-B₁₃H₁₃⁽²⁻⁾. Moreover, such a protocol successfully described the formation of *arachno*-4,5-C₂B₆H₁₁⁽⁻⁾ as the very final product of the first reaction. Analogous experimental transformations of *closo*-1,6-C₂B₈H₁₀ and *closo*-1,10-C₂B₈H₁₀, although attempted, were not successful. However, their transformations were explored through computations.

Keywords: carboranes; DFT; reaction pathways

1. Introduction

Polyhedral borane and heteroborane clusters are known for the presence of delocalized electron-deficient bonding [1,2] and characterized by forming three-center, two-electron (3c-2e) bonds. This bonding is quite different from organic chemistry that is dominated by classical two-center two-electron (2c-2e) bonds. The trigonal faces of boranes and carboranes are assembled to create three-dimensional shapes such as icosahedron and bicapped-square antiprism [2] appearing in *closo* systems. The preparation and subsequent reactivity of these clusters have been extensively studied by experiments [1,2]. In particular, the 12-vertex icosahedral *closo* clusters have been one of the main targets. In contrast to well-understood reaction mechanisms in organic chemistry, those in boron cluster chemistry can be very complex because there are very small energy differences between many intermediates and transition states. On that basis, the reaction of boron hydrides may involve many competing pathways [3]. For that reason, relatively little progress has so far been made in the understanding of the reaction mechanisms of boron hydrides and carboranes of various molecular shapes [4–6]. To our knowledge, the reaction pathways associated with ten-vertex *closo* carboranes, for instance *closo*-1,2-C₂B₈H₁₀ (see Scheme 1), have not yet been explored.



Scheme 1. Molecular diagrams of *closo-1,2-C₂B₈H₁₀*, *arachno-1,6,9-OC₂B₈H₁₃⁽⁻⁾* (**oP1-O**), and *arachno-1,6,9-NC₂B₈H₁₃⁽⁻⁾* (**oP1-N**) and the corresponding atomic numberings.

The $C_2B_8H_{10}$ molecular shape of a bicapped-square antiprism exists in seven positional isomers, only three of which (1,2-, 1,6- and 1,10-isomers) are known experimentally [2]. The most stable one is the 1,10-isomer and the least stable one is the 2,3-isomer [7]. The 1,6-isomer has recently been examined experimentally [8]. In addition, a new synthetic pathway for the preparation of the 1,2-isomer has also been outlined, including some mechanistic considerations [9]. Mutual isomerizations of all the possible *closo-C₂B₈H₁₀* have been studied computationally [10]. As to the observed reactivity of the 1,2-isomer, its direct *closo* to *arachno* transformations have been experimentally observed [11,12], with the resulting *arachno* structural motif being based on the hypothetical *closo-B₁₃H₁₃⁽²⁻⁾* as also seen from the corresponding atomic numberings (see also Scheme 1) [13]. Since no computational work has been reported in the area of the reactions of 10-vertex *closo* carboranes, we have undertaken a computational study of the experimentally known isomers of *closo-C₂B₈H₁₀* with the Lewis bases $OH^{(-)}$ and NH_3 . Both bases are hard in terms of the HSAB theory of acids and bases [14] with $OH^{(-)}$ being harder than NH_3 on the HSAB scale.

2. Methods

All of the stationary points in the reactions of *closo-1,2-*, *1,6-*, and *1,10-C₂B₈H₁₀* with $OH^{(-)}$ were optimized and frequencies were calculated at the SMD(water) [15,16]/B3LYP/6-311+G(2d,p) level, a model chemistry well-established for this class of materials [4–6]. The entries in Table 1 for B3LYP/6-311+G(2d,p) are single-point energies at SMD(water)/B3LYP/6-311+G(2d,p)-optimized geometries. The reactions of the same carborane with neutral NH_3 were optimized at the B3LYP/6-311+G(2d,p) level without taking solvation effects into account, which is quite reasonable for neutral species. Moreover, unlike the investigation of organic reaction mechanisms where the bonding is 2c–2e and bond-breaking reaction steps can cause the wave function to become unstable with respect to symmetry-breaking, in the investigation of electron deficient reactions, the bonding scheme fluidly changes between different patterns of multi-center bonding. While dynamic electron correlation is important (and described by the B3LYP approach used in this study), non-dynamic (i.e., static) electron correlation (caused by near degeneracy effects) is not important. All of the transition states were relaxed in terms of the application of the intrinsic reaction coordinate (IRC) approach at the SMD(water)/B3LYP/6-31+G(d) level for the reactions with $OH^{(-)}$ and at the B3LYP/6-31G(d) level for the reactions with NH_3 , and the structures obtained are very similar to those obtained with the 6-311+G(2d,p) basis set. In order to check the possible influence of dispersion corrections, the wB97XD/6-311+G(2d,p), model chemistry was also employed for some stationary points. All the computations were performed using Gaussian09, in which the above model chemistries and basis sets are incorporated [17].

Table 1. Solvation free energies (kcal·mol⁻¹), and free energies relative to the appropriate reference. The small “o” refers to ortho (1,2-) C₂B₈H₁₀. The capital letters “A”, “B”, “C”, etc. and “TS#” are related to individual intermediates and transition states, respectively. If there were two conformations possible, two letters are used to differentiate between them (e.g., oG/G’-O, oK/K’-O and oM/M’-O). The capital “-O” and “-N” distinguish between the reactions of OH⁽⁻⁾ and NH₃, respectively. Wherever the intermediate is relatively stable (and already isolated or possibly trappable), “P1”, “P2”, “P3”, etc. are used instead of “A”, “B”, “C”.

Notation	ΔG (solv) ¹	ΔG (aq,298K) ²	Notation	ΔG (solv) ¹	ΔG (aq,298K) ²
C ₂ B ₈ H ₁₀ + OH ⁽⁻⁾ ³			C ₂ B ₈ H ₁₀ + NH ₃ ⁴		
OH ⁽⁻⁾	-94.76		NH ₃	-3.67	
H ₂ O	-2.05		H ₂ BNH ₂	-1.24	
H ₂ BOH	-3.82		oTS1-N	-4.70	32.1
OBOH	-14.65		oA-N	-11.06	15.8
B(OH) ₃			oTS2-N	-0.43	50.3
oTS1-O	-53.74	27.2	oP1-N	-3.75	-1.3
oA-O	-46.19	2.0	oTS3-N	-0.64	43.8
oTS2O	-42.58	10.0	oB-N	-0.39	23.8
oB-O	-44.80	1.8	oTS4-N	-1.46	32.8
oTS3-O	-39.89	14.5	oC-N	-0.34	24.4
oP1-O	-40.16	-18.4	oTS5-N	-0.01	32.3
4,5-C ₂ B ₆ H ₁₁ ⁽⁻⁾	-39.67	-50.7	oD-N	0.27	31.2
oC-O	-41.59	-18.2	oTS6-N	0.81	39.5
oTS4-O	-45.21	18.5	P2-N	-3.48	7.3
oD-O	-47.70	-2.2	oTS7-N	-1.01	38.3
oTS5-O	-48.36	9.1	oE-N	-0.55	29.5
oE-O	-47.59	0.0	oTS8-N	0.49	36.4
oTS6-O	-47.61	0.2	oP3-N	-3.20	11.1
oF-O	-45.17	-1.2	oTS9-N	-3.06	32.1
oTS7-O	-43.15	8.8	oF-N	-3.30	29.7
oP2-O	-45.07	-18.8	oTS10-N	-6.51	29.8
oTS8-O	-58.47	6.2	oG-N	-2.08	25.1
oG-O	-63.94	1.6	oTS11-N	-2.74	35.0
oG’-O	-63.85	1.6	oH-N	-2.77	26.5
oTS9-O	-50.19	7.9	oTS12-N	-2.22	39.1
oH-O	-53.32	4.6	oI-N	-1.85	32.0
oTS10-O	-51.94	5.7	oTS13-N	-1.97	32.8
oI-O	-66.84	0.1	oP4-N	-2.27	-5.5
oJ-O	-60.59	-1.1			
oTS11-O	-58.96	-1.5			
oK-O	-48.64	-27.9			
oK’-O	-44.34	-26.8			
oTS12-O	-45.37	-19.5			
oL-O	-51.68	-26.9			
oM-O	-56.47	-28.4			
oM’-O	-53.96	-29.2			
oTS13-O	-58.13	-4.2			
4,5-C ₂ B ₆ H ₁₁ ⁽⁻⁾	-39.43	-41.7			

¹ Solvation free energies (the energy difference between B3LYP/6-311+G(2d,p) and SMD/B3LYP/6-311+G(2d,p) at 298.15 K (kcal·mol⁻¹). ² Relative free energies in kcal·mol⁻¹ (where the references are 1,2-C₂B₈H₁₀+OH⁽⁻⁾ for OH⁽⁻⁾ and 1,2-C₂B₈H₁₀+NH₃ for NH₃ reactions). The ΔG (aq,298K) and ΔG (solv) for 1,2-C₂B₈H₁₀ are 0.0 kcal·mol⁻¹ and -0.5 kcal·mol⁻¹, respectively. The solvation free energy of H₂O is taken from the experiment (-2.05 kcal·mol⁻¹). In some cases, H₂NBH₂ is added for mass balance. In the formation of C₂B₆H₁₁⁽⁻⁾, the comparison is made with respect to 1,2-C₂B₈H₁₀ + OH⁽⁻⁾+3H₂O. ³ Geometry optimizations and frequencies calculated at the SMD(water)/B3LYP/6-311+G(2d,p) level of theory. ⁴ Geometry optimizations and frequencies calculated at the B3LYP/6-311+G(2d,p) level of theory.

3. Results and Discussion

3.1. The Reaction with Hydroxides

The first part of the reaction of 1,2- $C_2B_8H_{10}$ with $OH^{(-)}$ is a quite straightforward process. This experimentally verified reaction, with the **oP1-O** final product, arachno-1,6,9- $OC_2B_8H_{13}^{(-)}$ (Scheme 1), proceeds through three transition states (TSs) and two intermediates, with the latter still bearing $OH^{(-)}$ (see Figure 1). The B-H-B bridge is a result of H migration to the B(7)–B(8) position in the final step of this reaction cascade. However, when one molecule of H_2O is added to **oP1-O**, the cluster further degrades and through seven TSs an intermediate **oI-O** is obtained, which is prone to further degradation, when another water molecule is added to the O–B–O–H chain through two hydrogen bonds. This initiation results, via selective degradation of B(3,6)-cage atoms, in the formation of arachno- $C_2B_6H_{11}^{(-)}$ through a number of TSs and intermediates, this arachno system being also isolated experimentally (see Figures 1 and 2 and Table 1) [18]. Note that the first barrier associated with **oTS1-O** was also examined with wB97XD/6-311+G(2d,p) and no significant difference from the B3LYP/6-311+G(2d,p) value was found, i.e., 24.9 kcal·mol⁻¹ vs. 27.2 kcal·mol⁻¹ as seen from Table 1. The potential energy surface attributed to the reaction of 1,6- $C_2B_8H_{10}$ + $OH^{(-)}$ was rather difficult to follow. Since this reaction was not observed experimentally, we moved this computational effort to Supplementary Materials (see Figures S1 and S2). The geometrical shape of the final product **mP3-O** bears a slight resemblance to the nido-11 vertex geometry, but not with the open pentagonal belt because the $OH^{(-)}$ group migrates through the entire process without any indication of the insertion of oxygen into the cage boron atoms (see Figure S1). The mechanism of the reaction of the 1,10 isomer with $OH^{(-)}$, also not observed experimentally, is even more complex. Interestingly, the final product (**pP1-O**, see Figures S3 and S4) of the latter reaction is of the same molecular shape, i.e., with a B–O–B bridge, as in the case of the reaction of 1,2- $C_2B_8H_{10}$ with $OH^{(-)}$ (**oP1-O**), but it originates through five TSs instead of three.

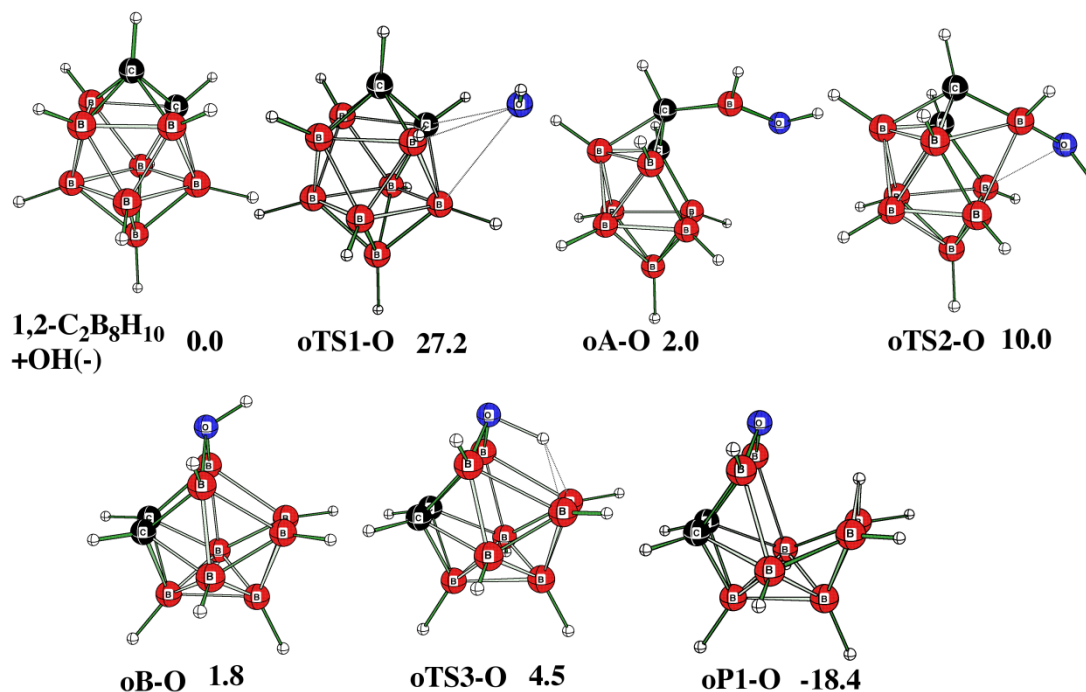


Figure 1. Cont.

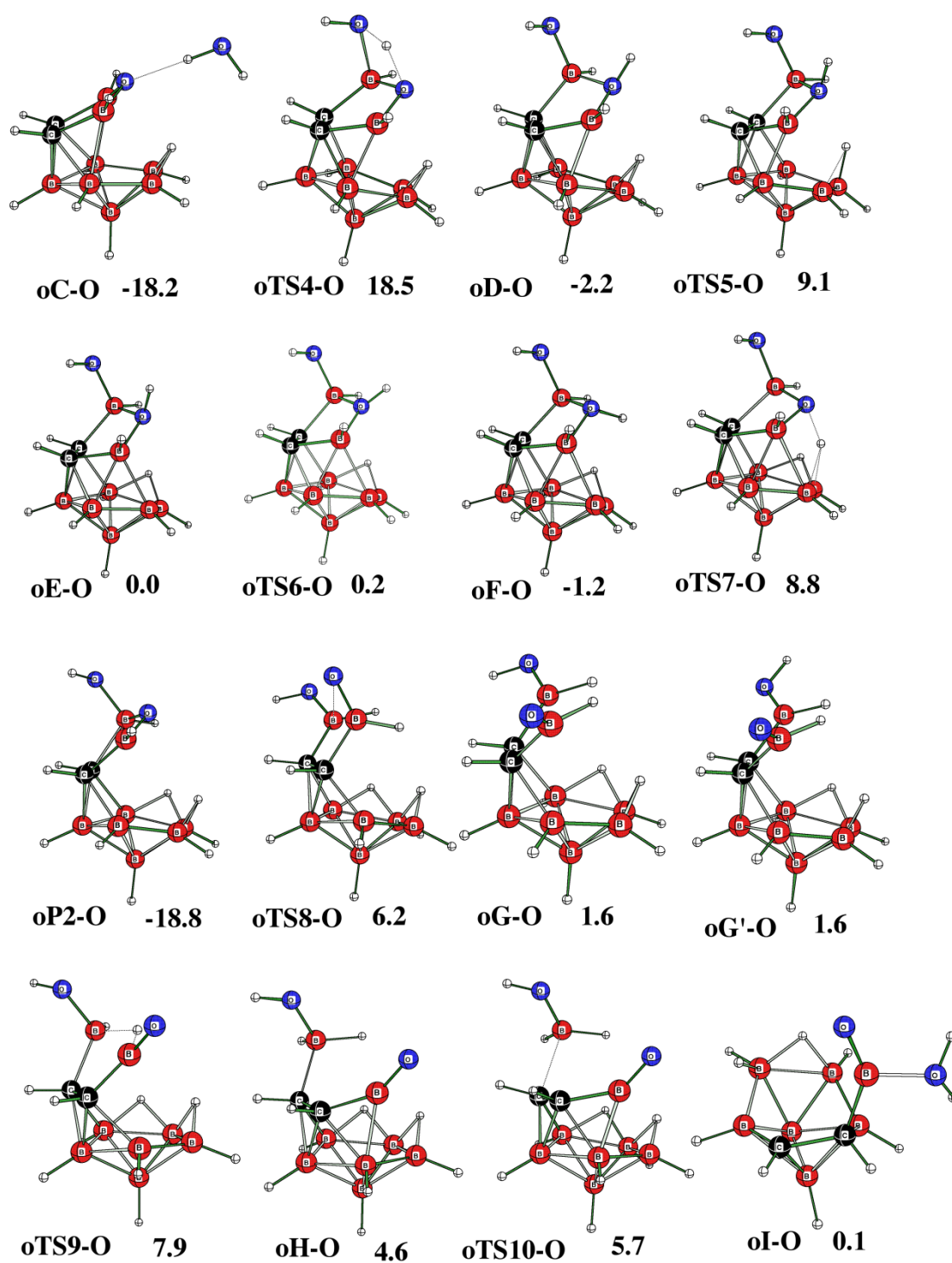


Figure 1. Cont.

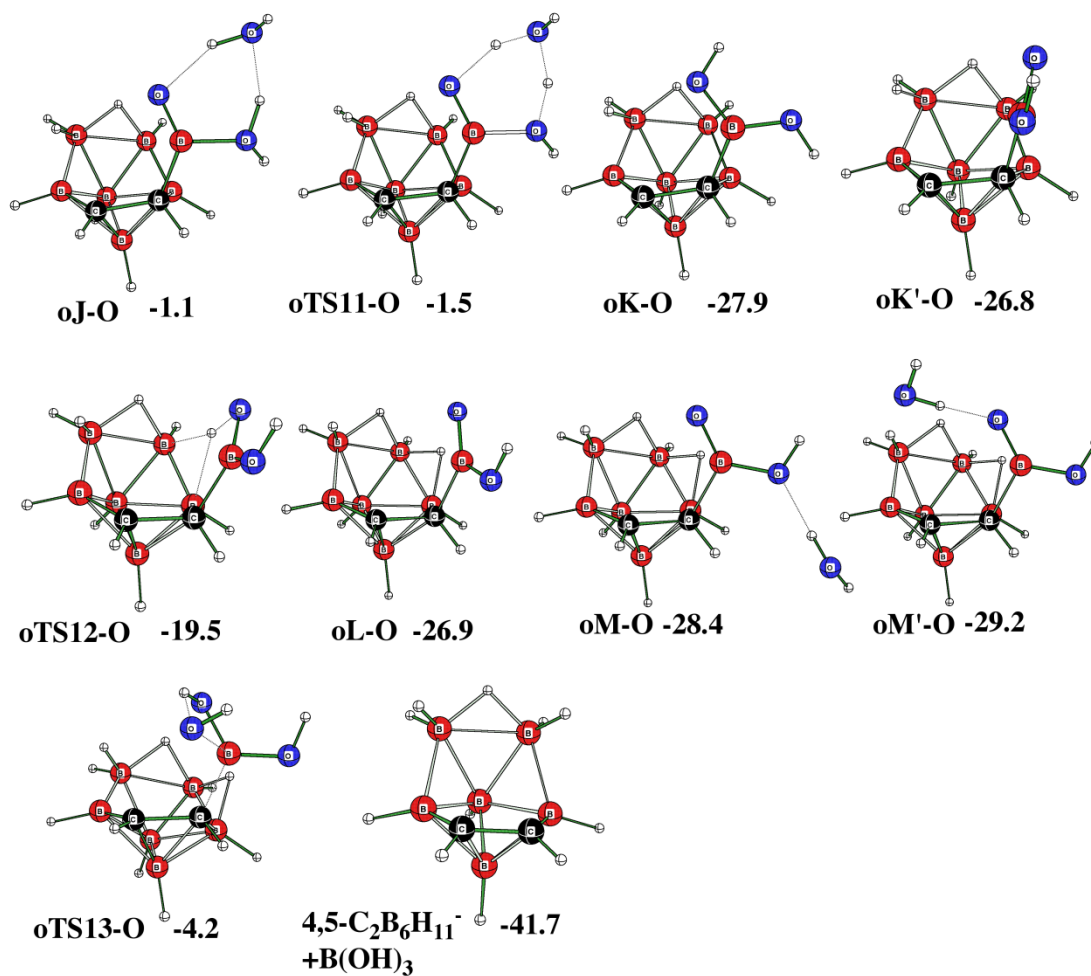


Figure 1. Individual stationary points as determined in the reaction pathway of the reaction of *closo*-1,2-C₂B₈H₁₀ with OH⁽⁻⁾.

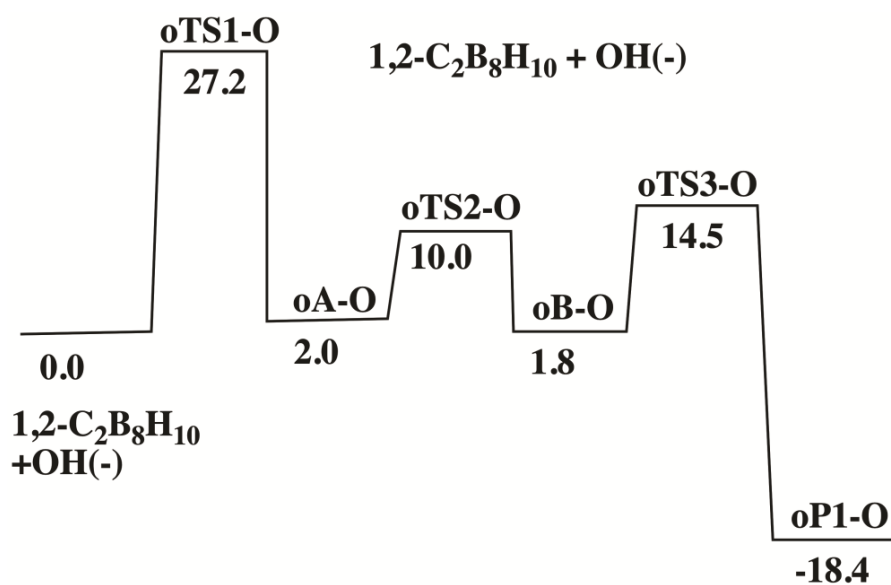


Figure 2. Cont.

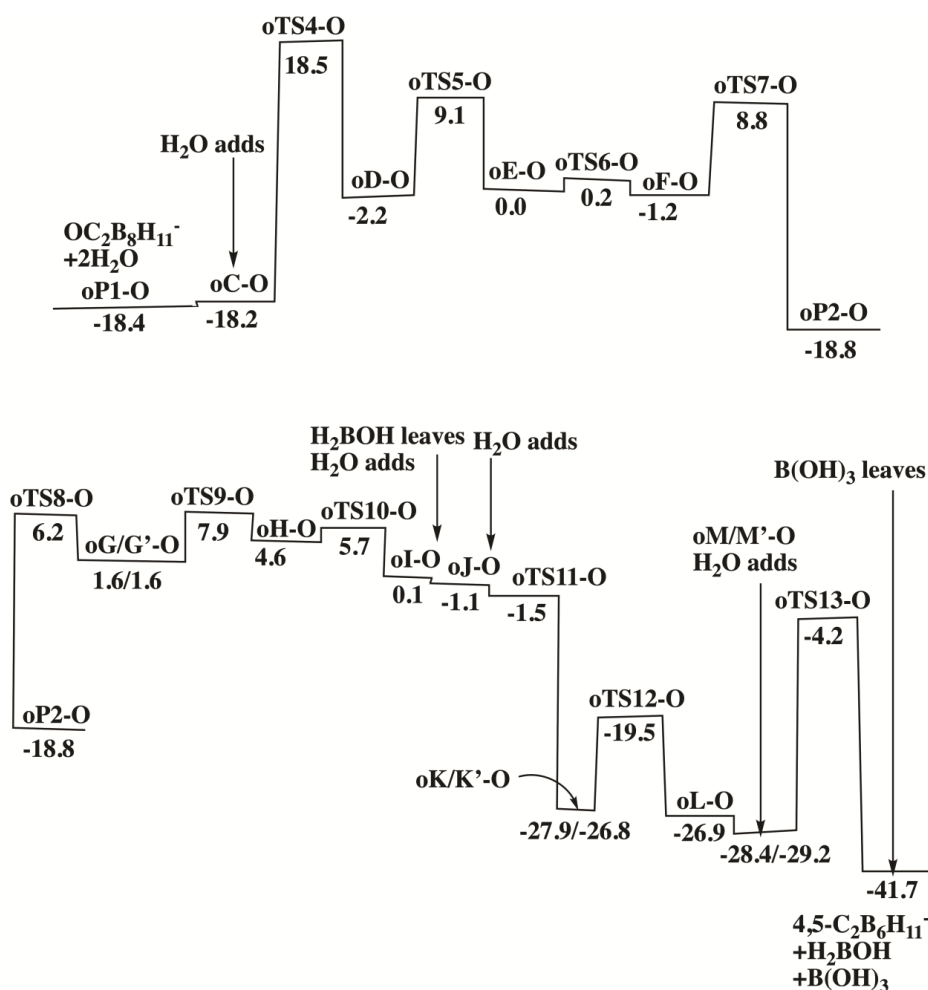


Figure 2. Relative free energies ($\text{kcal}\cdot\text{mol}^{-1}$) of the individual stationary points on the Potential Energy Surface (PES) of the reaction of *closo*-1,2- $\text{C}_2\text{B}_8\text{H}_{10}$ with OH^{-} (see Table 1 and Methods for details).

3.2. The Reaction with Amines

The reaction of *closo*-1,2- $\text{C}_2\text{B}_8\text{H}_{10}$ with NH_3 has been experimentally known to provide *arachno*-1,6,9- $\text{NC}_2\text{B}_8\text{H}_{13}$ (Scheme 1) [11,17]. The initiation of this reaction is based on the attack of NH_3 on the most positive boron within the cage, i.e., B(3), which forms a triangle with both C vertices. The highest free energy barrier ($50.3 \text{ kcal}\cdot\text{mol}^{-1}$) is **TS2-N**, through which the NH_3 group becomes NH_2 in the 1,6,9 isomer denoted as **oP1-N** in the reaction pathway (see Figures 3 and 4 and Table 1). However, this experimentally known part of the entire reaction (see above) occurs without any large intervening barriers and, consequently, the **oP1-N** isomer is obtained through two transition states and one intermediate. The same is apparently true for various amines of the $\text{R}_1\text{R}_2\text{NH}$ type [19]. This reaction proceeds through a series of intermediate steps to the known 1,8,11-isomer (**oP2-N**), experimentally available by another procedure [20]. To our knowledge, there is no experimental evidence of the conversion of **oP2-N** to **oP1-N**, although this process is computed to be exothermic ($\Delta G = -8.6 \text{ kcal}\cdot\text{mol}^{-1}$). Note that the experimentally detected *arachno*-1,6,9- $\text{NC}_2\text{B}_8\text{H}_{13}$ originates under less exothermic conditions than its oxygen analog. In analogy with the reaction of 1,2- $\text{C}_2\text{B}_8\text{H}_{10}$ with OH^{-} , we also examined the first barrier using $\text{wb97XD}/6\text{-}311+\text{G}(2\text{d},\text{p})$ and again no significant difference from the $\text{B3LYP}/6\text{-}311+\text{G}(2\text{d},\text{p})$ value was computed, i.e., $28.3 \text{ kcal}\cdot\text{mol}^{-1}$ vs. $32.1 \text{ kcal}\cdot\text{mol}^{-1}$ as provided by Table 1. When the 1,6,9-isomer (**oP1-N**) was examined computationally in terms of searching for another TS, i.e., **oTS7-N**, it isomerizes to a new isomer, **oP3-N**, through two TSs and one intermediate, **oE-N**, with the C–C bond remains intact as judged by a separation of 1.565 \AA . When the

C–C separation was increased, another TS and intermediate, i.e., **oTS9-N** and **oF-N**, respectively, were located with much longer C ... C separations of 2.409 and 2.774 Å, respectively. This significant geometrical change initiates a continuation of the reaction through other four subsequent TSs to the next known isomer, i.e., **oP4-N**. The reaction of the 1,6-isomers (see Figures S5 and S6) was a result of the simultaneous initial attack of NH₃ on B(3) and C(6); the N atom forms a cap above the B(2)B(3)C(6) triangle in the transition state with a free energy barrier of 34.6 kcal·mol⁻¹. The second free energy barrier was even higher, 52.0 kcal·mol⁻¹ and might account for the fact that this reaction does not occur experimentally. Interestingly, when the common product of the reactions of *closo*-1,2-C₂B₈H₁₀ and *closo*-1,6-C₂B₈H₁₀ with NH₃, i.e., **oP4-N**, is reached (see also Figure S5), both reactions proceed in the same way and *closo*-C₂B₇H₉ is obtained, where the two carbon atoms are separated from each other. Basically, there are five isomers of *closo*-C₂B₇H₉. The isomerization barrier between the most stable C_{2v} (C ... C separation) and the third most stable C₁ (C–C bond) forms is quite high (36 kcal·mol⁻¹). The high barrier is not unusual as isomerizations involving the C–C bond in carboranes often have rather high barriers. This type of *closo/closo* isomerization can also be described [21] in a more detailed way in terms of the consecutive double-Diamond-Square-Diamond (DSD) mechanism [10,22]. These two *closo* isomers have already been discussed by Schleyer [7] favoring the C_{2v}-symmetrical 4,5-isomer as well.

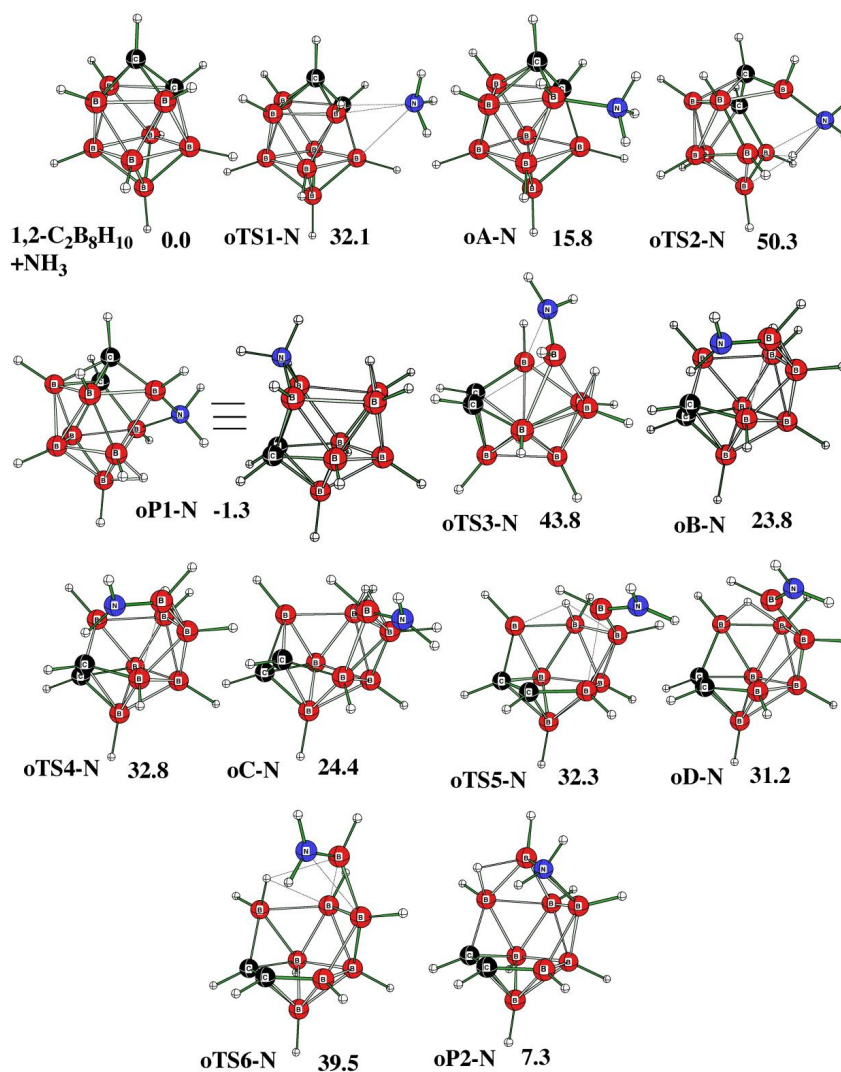


Figure 3. Cont.

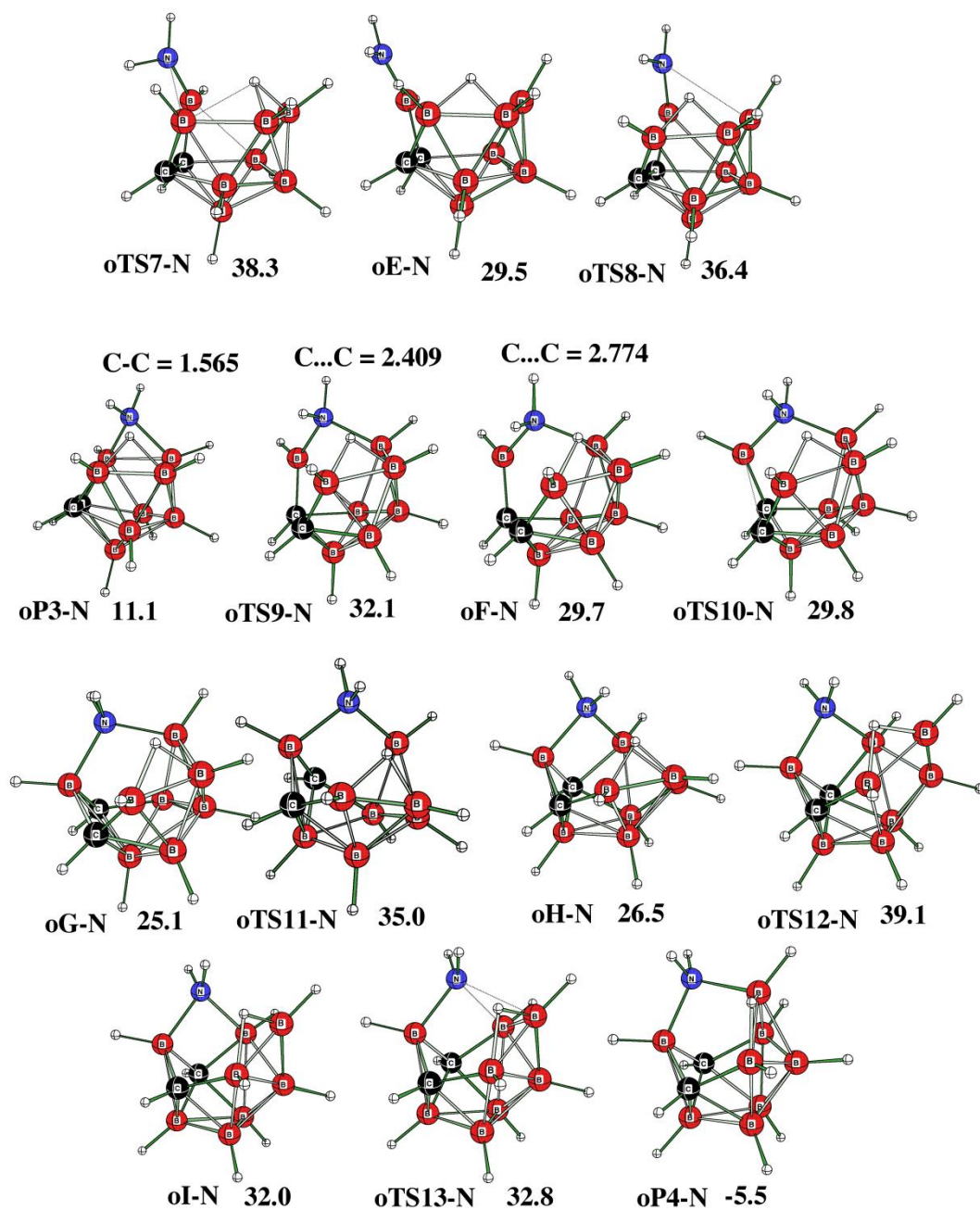


Figure 3. Individual stationary points on the PES of the reaction of *closo*-1,2-C₂B₈H₁₀ with NH₃.

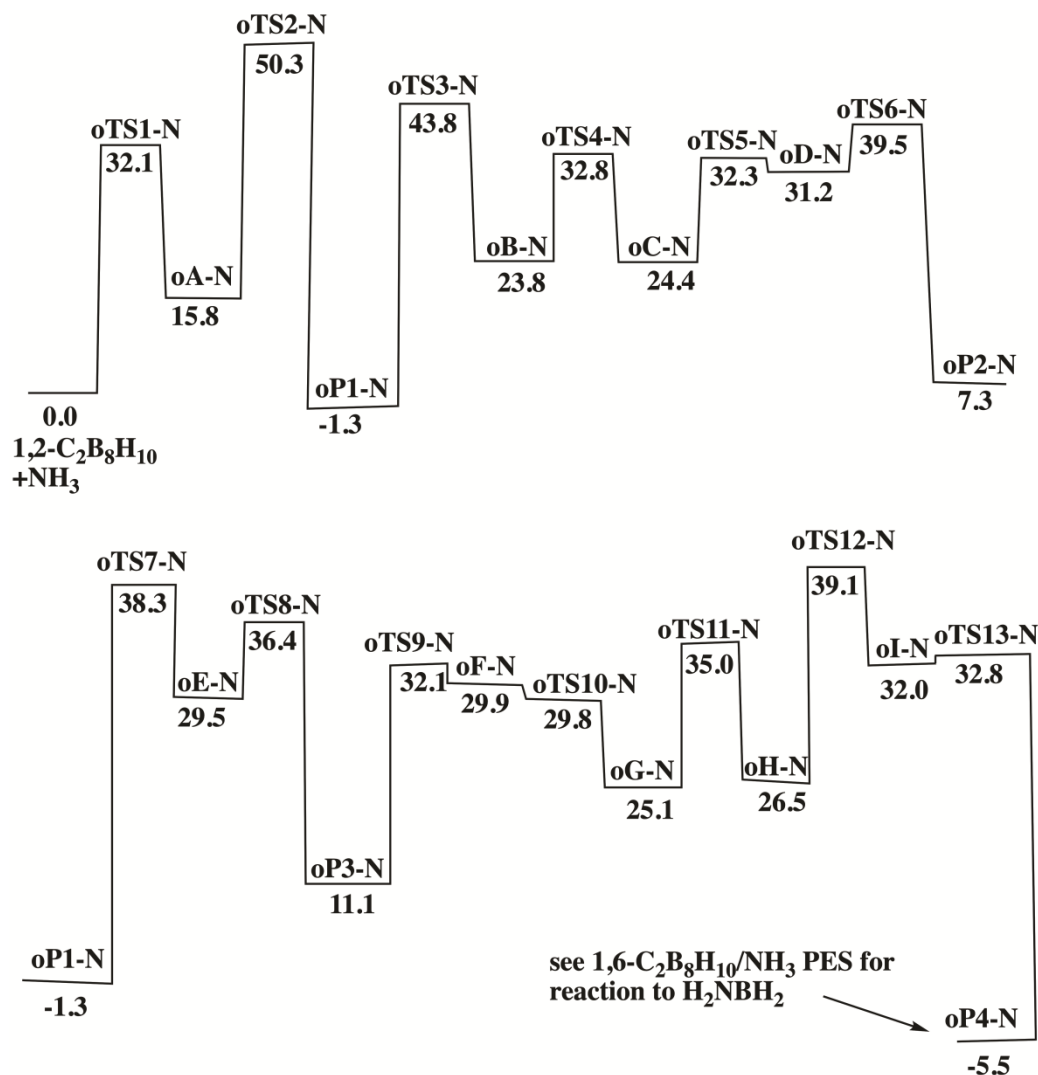


Figure 4. Relative free energies ($\text{kcal}\cdot\text{mol}^{-1}$) of the individual stationary points on the PES of the reaction of *closo*-1,2- $\text{C}_2\text{B}_8\text{H}_{10}$ with NH_3 (see Table 1 and Methods for details).

The reaction of the 1,10 isomer with NH_3 is rather complex and proceeds through a cascade of TSs. The initial attack of NH_3 simultaneously takes place at the boron atoms of both CB_4 hemispheres (**pTS1-N**) with an initial free energy barrier of more than $60 \text{ kcal}\cdot\text{mol}^{-1}$ and *closo*- $\text{C}_2\text{B}_7\text{H}_9$ originating as the final product in the endothermic reaction, which is entirely the same as above (see Figures S7 and S8). The experimental reaction of neither the 1,6- nor the 1,10-isomer of $\text{C}_2\text{B}_8\text{H}_{10}$ with NH_3 have been successfully carried out.

4. Conclusions

The reaction pathways of the experimentally known reactions of *closo*-1,2- $\text{C}_2\text{B}_8\text{H}_{10}$ with both $\text{OH}^{(-)}$ and NH_3 were computed using the DFT protocol. The final predicted products from the extensive search of the potential energy surfaces correspond to the same products detected experimentally. Both the *closo*-1,6- $\text{C}_2\text{B}_8\text{H}_{10}$ and the *closo*-1,10- $\text{C}_2\text{B}_8\text{H}_{10}$ isomers were allowed to react with the $\text{OH}^{(-)}$ and NH_3 bases, without any defined products being observed. Finally, this work represents a computational attempt to study the debor reaction, in contrast to the debor principle [23] (the successive elimination of vertices), where boron vertices are removed in the course of the reaction as illustrated by obtaining *arachno*- $\text{C}_2\text{B}_6\text{H}_{11}^{(-)}$ as the very final product from the reaction of *closo*-1,2- $\text{C}_2\text{B}_8\text{H}_{10}$ with $\text{OH}^{(-)}$.

Supplementary Materials: The following are available online at <http://www.mdpi.com/2073-4352/10/10/896/s1>: Figure S1: Individual stationary points as detected in the reaction pathway of the reaction of *closo*-1,6-C₂B₈H₁₀ with OH⁽⁻⁾, Figure S2: Relative free energies (kcal·mol⁻¹) of the individual stationary points on the PES of the reaction of *closo*-1,6-C₂B₈H₁₀ with OH⁽⁻⁾, Figure S3: Individual stationary points as detected in the reaction pathway of the reaction of *closo*-1,10-C₂B₈H₁₀ with OH⁽⁻⁾, Figure S4: Relative free energies (kcal·mol⁻¹) of the individual stationary points on the PES of the reaction of *closo*-1,10-C₂B₈H₁₀ with OH⁽⁻⁾, Figure S5: Individual stationary points as detected in the reaction pathway of the reaction of *closo*-1,6-C₂B₈H₁₀ with NH₃, Figure S6: Relative free energies (kcal·mol⁻¹) of the individual stationary points on the PES of the reaction of *closo*-1,6-C₂B₈H₁₀ with NH₃, Figure S7: Individual stationary points as detected in the reaction pathway of the reaction of 1,10-C₂B₈H₁₀ with NH₃, Figure S8: Relative free energies (kcal·mol⁻¹) of the individual stationary points on the PES of the reaction of *closo*-1,10-C₂B₈H₁₀ with NH₃, Table S1: Number of imaginary frequencies, zero-point energies (kcal·mol⁻¹), heat capacity correction (kcal·mol⁻¹), entropies (cal·mol⁻¹·K⁻¹), solvation free energies (kcal·mol⁻¹), and free energies relative to the appropriate reference. Small o, m, or p refer to ortho (1,2-), meta (1,6-), or para (1,10-)C₂B₈H₁₀, respectively. Capital letters “A”, “B”, “C”, etc. or “TS#” are related to individual intermediates or transition states, respectively. If there were two conformations possible, two letters are used to discern them (e.g., oG/G'-O, oK/K'-O, or oM/M'-O). Capital “-O” or “-N” distinguish between the reactions of OH(-) or NH₃, respectively. In cases where the intermediate is relatively stable (and already isolated or possibly trappable), “P1”, “P2”, “P3”, etc. is used instead of “A”, “B”, “C”. Table S2: Cartesian coordinates of all species in Table S1

Author Contributions: Computations, M.L.M., J.F., and D.H.; synthesis, J.H. All authors have read and agreed to the published version of the manuscript.

Funding: We thank the Czech Science Foundation for financial support (project no. 19-17156S). MLM thanks Auburn University for access to the HOPPER computer.

Conflicts of Interest: The authors declare no conflict of interest.

References

- Hnyk, D.; Wann, D.A. Boron: The Fifth Element. In *Challenges and Advances in Computational Chemistry and Physics*; Hnyk, D., McKee, M., Eds.; Springer: Dordrecht, The Netherlands, 2016; Volume 20, pp. 17–48.
- Grimes, R.N. *Carboranes*, 3rd ed.; Academic Press: Cambridge, MA, USA, 2016.
- McKee, M.L. Boron: The Fifth Element. In *Challenges and Advances in Computational Chemistry and Physics*; Hnyk, D., McKee, M., Eds.; Springer: Dordrecht, The Netherlands, 2016; Volume 20, pp. 121–138.
- McKay, D.; Macgregor, S.A.; Welch, A.J. Isomerisation of *nido*-[C₂B₁₀H₁₂]²⁻ Dianions: Unprecedented Rearrangements and New Structural Motifs in Carborane Cluster Chemistry. *Chem. Sci.* **2015**, *6*, 3117–3128. [[CrossRef](#)] [[PubMed](#)]
- Shameena, O.; Pathak, B.; Jemmis, E.D. Theoretical Study of the Reaction of B₂₀H₁₆ with MeCN: *Closo*/*Closo* to *Closo*/*Nido* Conversion. *Inorg. Chem.* **2008**, *47*, 4375–4382. [[CrossRef](#)] [[PubMed](#)]
- Štíbr, B.; Holub, J.; Bakardjiev, M.; Lane, P.D.; McKee, M.L.; Wann, D.A.; Hnyk, D. Unusual Cage Rearrangements in 10-Vertex *nido*-5,6-Dicarbaborane Derivatives: An Interplay between Theory and Experiment. *Inorg. Chem.* **2017**, *56*, 852–860. [[CrossRef](#)] [[PubMed](#)]
- Schleyer, P.V.R.; Najafian, K. Stability and Three-Dimensional Aromaticity of *closo*-Monocarborane Anions, CB_{n-1}H_n⁻, and *closo*-Dicarbaboranes, C₂B_{n-2}H_n. *Inorg. Chem.* **1998**, *37*, 3454–3457. [[CrossRef](#)] [[PubMed](#)]
- Bakardjiev, M.; Štíbr, B.; Holub, J.; Padělková, Z.; Růžička, A. Simple Synthesis, Halogenation, and Rearrangement of *closo*-1,6-C₂B₈H₁₀. *Organometallics* **2015**, *34*, 450–454. [[CrossRef](#)]
- Tok, O.L.; Bakardjiev, M.; Štíbr, B.; Hnyk, D.; Holub, J.; Padělková, Z.; Růžička, A. Click Dehydrogenation of Carbon-Substituted *nido*-5,6-C₂B₈H₁₂ Carboranes: A General Route to *closo*-1,2-C₂B₈H₁₀ Derivatives. *Inorg. Chem.* **2016**, *55*, 8839–8843. [[CrossRef](#)] [[PubMed](#)]
- Gimarc, B.M.; Ott, J.J. Isomerization of Carboranes C₂B₆H₁₈, C₂B₈H₁₀ and C₂B₉H₁₁ by the Diamond-Square-Diamond Rearrangement. *J. Am. Chem. Soc.* **1987**, *109*, 1388–1392. [[CrossRef](#)]
- Janoušek, Z.; Fusek, J.; Štíbr, B. The First Example of a Direct *closo* to *arachno* Cluster Expansion Reaction in Boron Cluster Chemistry. *J. Chem. Soc. Dalton Trans.* **1992**, 2649–2650. [[CrossRef](#)]
- Hnyk, D.; Holub, J. Handles for the Dicarbododecaborane Basket Based on [*arachno*-4,5-C₂B₈H₁₃]⁻: Oxygen. *Dalton Trans.* **2006**, 2620–2622. [[CrossRef](#)] [[PubMed](#)]
- Schleyer, P.V.R.; Najafian, K.; Mebel, A.M. The Large *closo*-Borane Dianions, B_nH_n²⁻ (n = 13–17) Are Aromatic, Why Are They Unknown? *Inorg. Chem.* **1998**, *37*, 6765–6772. [[CrossRef](#)] [[PubMed](#)]

14. For Example, Fleming, I. *Frontier Orbitals and Organic Chemical Reactions*; John Wiley and Sons: Chichester, Sussex, UK, 1976.
15. Marenich, A.V.; Cramer, C.J.; Truhlar, D.G. Universal Solvation Model Based on Solute Electron Density and on a Continuum Model of the Solvent Defined by the Bulk Dielectric Constant and Atomic Surface Tensions. *J. Phys. Chem. B* **2009**, *113*, 6378–6396. [[CrossRef](#)] [[PubMed](#)]
16. Marenich, A.V.; Cramer, C.J.; Truhlar, D.G. Performance of SM6, SM8, and SMD on the SAMPL1 test set for the prediction of small-molecule solvation free energies. *J. Phys. Chem. B* **2009**, *113*, 4538–4543. [[CrossRef](#)] [[PubMed](#)]
17. Frisch, M.J.; Trucks, G.W.; Schlegel, H.B.; Scuseria, G.E.; Robb, M.A.; Cheeseman, J.R.; Scalmani, G.; Barone, V.; Mennucci, B.; Petersson, G.A.; et al. *Gaussian 09, Revision, D.01*; Gaussian, Inc.: Wallingford, CT, USA, 2009.
18. Jelínek, T.; Štíbr, B.; Heřmánek, S.; Plešek, J. A New Eight-Vertex arachno-Dicarbaborane anion, $[4,5-C_2B_6H_{11}]^-$. *J. Chem. Soc. Chem. Commun.* **1989**, 804–805. [[CrossRef](#)]
19. Janoušek, Z.; Dostál, R.; Macháček, J.; Hnyk, D.; Štíbr, B. The First Member of the Eleven-Vertex Azadiborane Series, 1,6,9-NC₂B₈H₁₃ and its N-alkyl Derivatives. *Dalton Trans.* **2006**, 4664–4671. [[CrossRef](#)] [[PubMed](#)]
20. Plešek, J.; Štíbr, B.; Hnyk, D.; Jelínek, T.; Heřmánek, S.; Kennedy, J.D.; Hofmann, M.; Schleyer, P.V.R. Dicarbaheteroborane Chemistry. Representatives of Two Eleven-Vertex Dicarbaazaundecaborane Families: Nido-10,7,8-NC₂B₈H₁₁, Its N-Substituted Derivatives, and arachno-1,8,11-NC₂B₈H₁₃. *Inorg. Chem.* **1998**, *37*, 3902–3909. [[CrossRef](#)] [[PubMed](#)]
21. Ceulemans, A.; Goijens, G.; Nguyen, M.T. C₂B₇H₉: Snapshots of a Rearranging Carborane. *J. Am. Chem. Soc.* **1994**, *116*, 9395–9396. [[CrossRef](#)]
22. Lipscomb, W.N. Framework Rearrangement in Boranes and Carboranes. *Science* **1966**, *153*, 373–378. [[CrossRef](#)] [[PubMed](#)]
23. Wade, K. Structural and Bonding Patterns in Cluster Chemistry. *Adv. Inorg. Chem. Radiochem.* **1976**, *18*, 1–66.



© 2020 by the authors. Licensee MDPI, Basel, Switzerland. This article is an open access article distributed under the terms and conditions of the Creative Commons Attribution (CC BY) license (<http://creativecommons.org/licenses/by/4.0/>).